Received: 6 July 2016 | Accepted: 31 August 2016

DOI: 10.1111/jace.14565

ORIGINAL ARTICLE

Journal of the American Ceramic Society

Local structure of network modifier to network former ions in soda-lime alumino-borosilicate glasses

Ming-Tai Ha | Stephen H. Garofalini

Materials Science and Engineering, Rutgers University, Piscataway, New Jersey

Correspondence
Stephen H. Garofalini, Materials Science and Engineering, Rutgers University, Piscataway, NJ.
Email: shg@glass.rutgers.edu

Abstract

The structure of soda-lime alumino-borosilicate glass was studied using molecular dynamics simulations of samples of varying compositions containing ~20 000 atoms each. Pair distribution functions (PDFs) of cations to oxygen were used for comparison to available experimental data to evaluate consistency between simulations and experiment. Additional PDFs and coordination of the network forming cations (Al/B/Si) to network modifiers (Ca/Na) were examined, which is difficult to measure experimentally. The results are consistent with available experimental data regarding cation-oxygen bond lengths and network former to oxygen coordination numbers. Si and Al are predominantly 4-coordinated, with a small concentration of overcoordinated species similar to experimental data. B varied as 3-coordinated, BO_3, and 4-coordinated, BO_4, as a function of the amount of Ca^{2+} and Na^+ present, the ratio of Al_2O_3 to B_2O_3, and the fictive temperature of the sample, similar to experimental data. The simulations provide new information regarding the locations on the network modifiers to the +3 cations, Al and B. For instance, one Al ion can have multiple Na within 4 Å, but also the Na can be within 4 Å of several +3 cations. Such results would indicate a greater complexity of local structure that goes beyond the stoichiometric one +1 modifier ion near one +3 network former or one +2 modifier near two +3 formers in tetrahedral sites.

KEYWORDS

alumino-borosilicates, amorphous, atomistic simulation, soda-lime-silica, structure

1 | INTRODUCTION

Aluminoborosilicate glasses are widely used in many technologies such as commercial glasses, fiber glass, photochromic glasses, glazes, and the sequestration of radioactive waste.[1-5] For instance, E-Glass is a type of alumino-borosilicate glass with a particular range of compositions and E-glass fibers are used in composites for their ability to maintain their strength properties over a wide range of conditions.[6-8] Extensive effort has been made to document the properties of various alumino-borosilicate glass compositions, as well as efforts to explore the structure of alumino-borosilicate glasses.[9-15]

Silica glass is composed of SiO_4 tetrahedra that are connected to create an amorphous network. Introducing alkali and alkaline-earth elements into a pure silica structure, the cations act as modifiers and reduce the connectivity in the tetrahedral network. When introducing Al_2O_3 and B_2O_3 into the continuous random silicate network formed by the corner-sharing SiO_4 tetrahedral network, the Al and B atoms replace the Si, forming mostly AlO_4 tetrahedra and trigonal BO_3 and BO_4 tetrahedra.[14] However, charge compensation of these +3 cations in the +4 Si network tetrahedral site is required and alkali and alkaline-earth cations can provide such compensation. When modifiers are added to borosilicate glasses the formation of tetrahedral boron

(BO_4) over trigonal boron (BO_3) occurs up to about 40% alkali,[15,16] depending upon modifier and silica content, with formation of more nonbridging oxygens (NBO). Moreover, different cations alter the structure of the alumino-borosilicate glass because of their different cation field strengths. Wu and Stebbins reported that Ca^{2+} more strongly promotes the formation of NBO than K^+ because of its higher field strength.[14] The structure of borosilicate glass with modifiers Na^+ and K^+ is no different from borosilicate with only one of these two modifiers.[17] Higher cation field strengths also increase the formation of five coordinated Al (^{5}Al) in aluminosilicate glasses.[18] However, in the metaluminous region, cation charge influences NBO formation.[18]

Although nuclear magnetic resonance (NMR) studies have provided excellent information regarding the structure of alumino-borosilicate glass and cation-anion distances, it is difficult to determine the interaction distance and coordination numbers between Al/B/Si to modifiers such as Na and Ca. Simulations on calcium in aluminosilicate glasses have been performed to determine pair distribution functions (PDFs) of Al/Si–Ca.[12,19] However, these involved very small system sizes and, in the classical simulations used in those references, an inaccurate and overly restrictive 3-body term on the Al was used in comparison to the more reliable version presented below.[20] A more extensive analysis of more complex systems is presented here, with additional information indicating the coordination of the modifiers to the 3^+ network formers, Al and B.

The aim of this paper is to analyze the structure of alumino-borosilicate glasses of varying compositions using molecular dynamics simulations to determine the bond or interaction distance between different atomic species and the coordination of the Al/B/Si–Ca/Na atom pairs to provide information on the behavior of modifiers on the alumino-borosilicate glass structure.

2 | COMPUTATIONAL PROCEDURE

The multibody potential of the following form is used,

$$V = \sum_{i \neq j} V_{ij}^{\mathrm{BMH}} + \sum_{i \neq j \neq k} V_{jik}^{3-\mathrm{body}} \quad (1)$$

where V_{ij}^{BMH} represents the Born-Mayer-Huggins (BMH) pair potential term, and $V_{jik}^{3-\mathrm{body}}$ represents the three-body term. The BMH two-body interactions are calculated using the following form,

$$V_{ij}^{\mathrm{BMH}} = A_{ij} \exp\left(\frac{-r_{ij}}{\rho_{ij}}\right) + \left(\frac{z_i z_j e^2}{r_{ij}}\right) \mathrm{erfc}\left(\frac{r_{ij}}{\beta_{ij}}\right) \quad (2)$$

and the optimal values of the parameters A_{ij}, β_{ij}, and ρ_{ij} for each pair were determined in previous work and are given in Table 1.[21,22] z_i and z_j represent the full charge of the ions i and j and e represents the elementary charge. r_{ij} denotes the separation between the ions i and j. The complementary error function (erfc) in the Coulomb term of the BMH equation behaves such that the pair potential function is zero when the separation of the ions is greater than 5.5 Å.

The three-body term is included to account for the partial covalency of Si–O, Al–O, and B–O bonding. These interactions are described by the following formulas:If r_{ij}<-R_{ij} and r_{ik}<R_{ik},

$$V_{jik}^{3-\mathrm{body}} = \lambda_{ij}^{\frac{1}{2}} \lambda_{ik}^{\frac{1}{2}} * \exp\left[\frac{\gamma_{ij}}{(r_{ij} - R_{ij})} + \frac{\gamma_{ik}}{(r_{ik} - R_{ik})}\right] \Theta_{jik}, \quad (3)$$

else,

$$V_{jik}^{3-\mathrm{body}} = 0 \quad (4)$$

The angular component Θ_{jik} for Si/A/B–O–Si/Al/B and O–Si/B–O is given by,

$$\Theta_{jik} = \left(\cos\theta_{jik} - \cos\theta_{jik}^0\right)^2 \quad (5)$$

and the angular component for O–Al–O is given by,

$$\Theta_{jik} = \left(\left(\cos\theta_{jik} - \cos\theta_{jik}^0\right) \sin\theta_{jik} \cos\theta_{jik}\right)^2 \quad (6)$$

where θ_{jik} is the angle formed by the ions j, i, and k with the ion i as the vertex. Even though the $\cos\theta_{jik}^0$ term in Equation (6) is 109.5°, the additional sine and cosine terms enable Equation (6) to have multiple minima that add more flexibility and reliability for Al bonding. The parameters λ_{ij}, γ_{ij}, R_{ij}, and θ_{jik}^0 are given in Table 2. Note that there are no three-body terms centered on Ca or Na because bond directionality is not expected. This potential form, with the different 3-body terms (Equations 5 and 6) has been used previously for simulations of silica, alumina, and glassy silicates and aluminosilicates.[20,23-26] While some potentials use very stiff 3-body terms, the 3-body forms shown here are relatively soft and are not overly restrictive. Hence, Equation (6) for Al allowed for the use of this one form for the accurate structure of γ-Al_2O_3, where the Al is in both 4- and 6-coordination, while also giving accurate structure for α-Al_2O_3, where Al is in 6 coordination[23].

Constant volume and temperature simulations were performed on 14 samples with compositions given in Table 3. The first eight compositions chosen were based on previous work that had used the same compositions but smaller system sizes.[27] Two densities were used for these glasses to mimic different fictive temperatures for the same compositions: LowEG (1-4) had densities of 2.30, 2.40, 2.45, 2.40 g/cm^3, respectively, and the EG (1-4) had a density of 2.55 g/cm^3. The compositions of the last six samples in

TABLE 1 Parameters for modified BMH pair potential

Atom	O	Na	Ca	B	Al	Si
Charge (z_i)	−2	+1	+2	+3	+3	+4
Atom Pair	A_{ij}		β_{ij}(pm)		ρ_{ij}(pm)	
O-O	0.0725		234		29	
Si-Si	0.1877		230		29	
Al-Al	0.0500		235		29	
B-B	0.1100		230		29	
Ca-Ca	0.7000		230		29	
Na-Na	0.2159		230		29	
Si-Al	0.2523		233		29	
Si-B	0.2000		230		29	
Si-Ca	0.2215		230		29	
Si-Na	0.2001		230		29	
Al-B	0.0450		230		29	
Al-Ca	0.2420		230		29	
Al-Na	0.2178		230		29	
B-Ca	0.1930		230		29	
B-Na	0.1740		230		29	
Si-O	0.2962		234		29	
Al-O	0.2490		234		29	
B-O	0.1400		234		29	
Ca-O	0.5700		234		29	
Na-O	0.3195		234		29	

TABLE 2 Three-body potential parameters

Atom triplet	λ_{ij} (fJ)	γ_{ij} (Å)	R_{ij} (Å)	θ_{jik} (°)
Si/Al/B–O–Si/Al/B	0.001	2.0	2.6	109.5
O–Si/Al–O	0.024	2.8	3.0	109.5
O–B–O	0.024	2.8	3.0	120.0

Table 3 were chosen to characterize the structure of alumino-borosilicate glasses with controlled variation in the composition and also have a density of 2.55 g/cm^3.

A melt-quench procedure was used to produce the alumino-borosilicate samples. Each glass sample was formed with simulations in the following order with a time step of 0.1 fs: 100 K for 1 ps; at 8000 K for 10 ps; at 6000 K for 20 ps, 50 ps at each temperature for 5000, 4000, 3000, and 2000 K; at 1000 K for 20 ps; at 300 K for 10 ps. While the quench rate is fast (~10^{13} K/s) recent work by Adelstein and Lordi showed that quench rate differences from 10^{11} to 10^{14} K/s did not show any significant difference in structure.[28] The size of each sample calculated was based on the density of the glass and the number of atoms in the sample. Three-dimensional periodic boundaries were imposed on the systems.

TABLE 3 Composition of the alumino-borosilicate glass samples

Name	SiO_2 (mol%)	Al_2O_3 (mol%)	B_2O_3 (mol%)	CaO (mol%)	Na_2O (mol%)	Total number of atoms
LowEG1	68.6	2.89	8.46	10.5	9.51	20 000
LowEG2	69.6	5.86	4.29	10.6	9.63	20 001
LowEG3	59.6	2.93	17.2	10.6	9.63	20 000
LowEG4	62.2	12.2	4.47	11.1	10.0	20 001
EG1	68.6	2.89	8.46	10.5	9.51	20 000
EG2	69.6	5.86	4.29	10.6	9.63	20 001
EG3	59.6	2.93	17.2	10.6	9.63	20 000
EG4	62.2	12.2	4.47	11.1	10.0	20 001
EGA5B15	60	5	15	10	10	19 998
EGA10B10	60	10	10	10	10	19 998
EGA15B5	60	15	5	10	10	19 998
EGCa20	60	10	10	20	0	20 000
EGCa10	70	10	10	10	0	19 998
EGNa20	60	10	10	0	20	19 998
EGNa10	70	10	10	0	10	19 998

3 | RESULTS AND DISCUSSION

The radial distribution function was calculated for individual cation-oxygen pairs (Si/Al/B/Ca/Na–O), and B–Ca/Na, and Al–Ca/Na interactions, creating PDFs. The positions of the peaks of each pair for all samples are given in Table 4 as well as experimental results. The Si–O bond is 1.61 Å and matches well with results from Greaves et al.[29] Figure 1 shows the PDFs of the Si–O bonds for six compositions; the rest of the compositions have very similar PDFs (see Supporting Information). The mean coordination for the Si–O bond for every sample, found on Tables 5-11, confirms the SiO_4 tetrahedral network and also shows there is a small percentage of 5-coordinated Si, indicating the presence of SiO_5. In those compositions with Na concentration in excess of Al, the concentration of 5-coordinated Si is slightly above 1%; otherwise it is below 0.6%. Both are higher concentrations of the SiO_5 than we normally find for Si in pure silica using this potential. 5-coordinated Si has been observed in NMR studies following the predictions from MD simulations.[30,31] Samples EGA5B15, EGA10B10, and EGA15B5 indicate that as the ratio of Al_2O_3/B_2O_3 increases, the presence of SiO_5 increases. There is otherwise no correlation between the presence of 5-coordinated Si and ratio of Al_2O_3/B_2O_3 found in the other samples shown in the Supporting Information.

The Al–O bond is 1.705-1.715 Å, similar to that reported in aluminosilicate zeolites,[32] but lower than the 1.74-1.77 Å reported in several experiment studies.[33-35] Figure 2 shows the PDFs of the Al–O bonds for six

TABLE 4 Bond lengths in aluminoborosilicate glass systems of ~20 000 atoms at 300 K, acquired by using $g_{ab}(r)$

(in Å)	Al-Ca	Al-Na	B-Ca	B-Na	AlO_4	BO_3	BO_4	Ca-O	Na-O	Si-O	Si-Ca	Si-Na
Ref	3.37[a,b]	N/A	N/A	3.20[c]	1.715[d],1.77[k],1.76[m],1.74[n]	1.37[e], 1.37[l]	1.48[f], 1.46[l]	2.50[a],2.36[b],2.45[g],2.35[m]	2.52-2.60[h]	1.60- 1.61[j]	3.40[b], 3.50[i]	3.40[i]
MD												
LowEG1	3.23	3.34	3.16	3.17	1.715	1.365	1.46	2.38	2.7	1.61	3.47	3.44
LowEG2	3.29	3.26	3.18	3.18	1.71	1.355	1.455	2.39	2.67	1.61	3.44	3.42
LowEG3	3.25	3.3	3.17	3.22	1.715	1.36	1.455	2.51	2.65	1.61	3.43	3.41
LowEG4	3.21	3.27	3.21	3.25	1.705	1.345	1.45	2.48	2.64	1.61	3.44	3.42
EG1	3.24	3.27	3.16	3.17	1.715	1.365	1.455	2.49	2.64	1.61	3.44	3.41
EG2	3.25	3.27	3.15	3.2	1.715	1.355	1.455	2.44	2.63	1.61	3.42	3.39
EG3	3.28	3.29	3.16	3.19	1.715	1.355	1.45	2.51	2.66	1.61	3.39	3.4
EG4	3.23	3.26	3.15	3.23	1.715	1.35	1.45	2.49	2.65	1.61	3.43	3.42
EGA5B15	3.24	3.3	3.2	3.16	1.715	1.36	1.455	2.46	2.61	1.61	3.4	3.35
EGA10B10	3.25	3.29	3.19	3.15	1.71	1.355	1.445	2.45	2.61	1.61	3.41	3.36
EGA15B5	3.23	3.3	3.18	3.18	1.71	1.35	1.45	2.47	2.61	1.61	3.43	3.36
EGCa10	3.26	N/A	3.19	N/A	1.71	1.355	N/A	2.51	N/A	1.61	3.46	N/A
EGCa20	3.24	N/A	3.18	N/A	1.715	1.355	1.435	2.47	N/A	1.61	3.45	N/A
EGNa10	N/A	3.29	N/A	3.16	1.715	1.35	N/A	N/A	2.65	1.61	N/A	3.4
EGNa20	N/A	3.24	N/A	3.13	1.71	1.365	1.445	N/A	2.58	1.61	N/A	3.32

[a12] [Computation].
[b19] [Computation].
[c44] [Computation].
[d45] [Computation].
[e39] [Computation].
[f38] [Experiment].
[g46] [Computation].
[h47] [Experiment].
[i34] [Computation].
[j29] [Experiment].
[k33] [Experiment].
[l37] [Experiment].
[m34] [Experiment].
[n35] [Experiment].

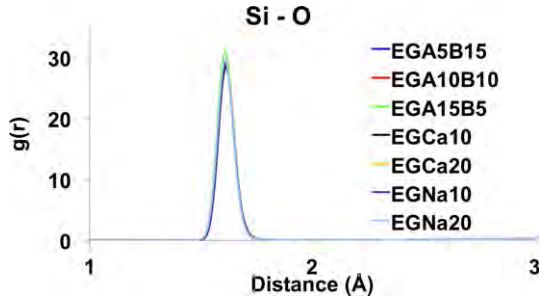

FIGURE 1 The Si–O bond distances at 300K of samples EGA5B15, EGA10B10, EGA15B5, EGCa20, EGCa10, EGNa20, EGNa10 [Color figure can be viewed at wileyonlinelibrary.com]

compositions; the rest of the compositions have very similar PDFs as shown in the supplementary information. Also, the mean coordination of Al–O indicates the presence of 5-coordinated Al (AlO_5), and a minor (<0.5%) 6-coordinated Al (AlO_6). Such overcoordinated Al has been observed experimentally.[11,18] Of the EGA5B15, EGA10B10, and EGA15B5 samples, EGA10B10 has the lowest percentage of AlO_4 and the highest percentage of AlO_5 and AlO_6. Also, the percentage of Al atoms forming AlO_5 correlates with the increasing density, which is an inverse correlation with the fictive temperature of the glass, as shown in the supplementary information regarding the difference in the "LowEG1-4" series with low density and the "EG1-4" series. Such a result is consistent with experiments performed by Wu and Stebbins.[36]

Figure 3 shows that the PDF of the B–O bond has two peaks, which correspond to the bond distances of BO_3 and BO_4 between 1.37 and 1.46-1.48 Å, respectively.[37-39] Wu and Stebbins[36] showed that the BO_3/BO_4 ratio can be changed by fixing the presence of a network modifying cation (Na^+, Ca^{2+}) and by varying the B_2O_3 in a sample; the Al_2O_3 mol% in the glass was fixed throughout. Namely, for alumino-borosilicate glasses, the ratio of BO_3/BO_4 decreases with increasing Na_2O (decreasing CaO) and with increasing B_2O_3 (decreasing Al_2O_3), depending on the Al_2O_3/B_2O_3 ratio. Our simulation extends that result by comparing three glass samples, namely EGA5B15, EGA10B10, and EGA15B5, with 10 mol% CaO and Na_2O each and a varying ratio of Al_2O_3/B_2O_3. From this it can be shown how the structure changes when both modifier cations are included. Figure 3A indicates that the ratio of Al_2O_3/B_2O_3 affects the ratio of BO_3/BO_4, showing decreased BO_4 with increasing Al_2O_3 with a constant

TABLE 5 Cutoff and average radius, mean coordination, and coordination distribution of EGA5B15 at 300 K

EGA5B15	Cutoff *R* (Å)	Avg *R* (Å)	Avg Coord	0	1	2	3	4	5	6	7	8
Si–O	1.9	1.62	4.01	0	0	0	0	98.60	1.40	0	0	0
Al–O	2.3	1.76	4.26	0	0	0	0	74.92	24.26	0.83	0	0
B–O	1.9	1.44	3.60	0	0	0	39.66	60.34	0	0	0	0
Al–Ca	4.6	3.53	1.34	21.62	39.27	26.07	9.74	3.14	0.17	0	0	0
Al–Na	4.76	3.66	2.43	6.60	19.31	25.91	28.05	13.53	5.61	0.99	0	0
B–Ca	4.3	3.41	1.06	28.99	43.45	21.45	5.17	0.88	0.06	0	0	0
B–Na	4.52	3.51	2.13	7.04	24.75	32.89	22.55	9.90	2.42	0.44	0	0
Si–Ca	4.58	3.68	0.97	35.04	39.38	19.80	4.76	0.88	0.14	0	0	0
Si–Na	4.68	3.71	2.19	8.25	22.74	30.23	23.87	11.30	2.94	0.63	0	0

TABLE 6 Cutoff and average radius, mean coordination, and coordination distribution of EGA10B10 at 300 K

EGA10B10	Cutoff *R* (Å)	Avg *R* (Å)	Avg Coord	0	1	2	3	4	5	6	7	8
Si–O	1.9	1.62	4.01	0	0	0	0	99.34	0.66	0	0	0
Al–O	2.3	1.76	4.25	0	0	0	0.08	75.41	24.01	0.50	0	0
B–O	1.9	1.43	3.53	0	0	0	46.70	53.30	0	0	0	0
Al–Ca	4.58	3.53	1.29	23.02	38.70	26.49	9.65	1.98	0.17	0	0	0
Al–Na	4.74	3.64	2.27	7.43	21.86	31.52	21.53	12.05	4.29	1.07	0.25	0
B–Ca	4.34	3.42	1.03	32.34	38.78	22.94	5.53	0.41	0	0	0	0
B–Na	4.5	3.52	1.97	10.81	26.16	30.45	22.77	7.92	1.73	0.17	0	0
Si–Ca	4.56	3.67	0.95	36.17	39.88	17.85	5.17	0.83	0.11	0	0	0
Si–Na	4.7	3.72	2.20	7.62	23.21	29.98	24.48	11.22	2.92	0.47	0.11	0

TABLE 7 Cutoff and average radius, mean coordination, and coordination distribution of EGA15B5 at 300 K

EGA15B5	Cutoff *R* (Å)	Avg *R* (Å)	Avg Coord	0	1	2	3	4	5	6	7	8
Si–O	1.9	1.62	4.00	0	0	0	0	99.64	0.36	0	0	0
Al–O	2.3	1.76	4.11	0	0	0	0.07	89.39	10.01	0.53	0	0
B–O	1.9	1.42	3.47	0	0	0	52.97	47.03	0	0	0	0
Al–Ca	4.6	3.55	1.20	24.37	41.91	24.70	7.37	1.54	0.11	0	0	0
Al–Na	4.7	3.63	2.24	7.15	22.22	29.70	25.19	12.10	3.19	0.39	0	0
B–Ca	4.32	3.40	1.07	29.04	44.06	19.47	6.11	1.16	0.17	0	0	0
B–Na	4.5	3.52	1.83	12.21	28.05	32.67	20.13	5.45	1.32	0.17	0	0
Si–Ca	4.6	3.69	0.99	33.70	39.91	21.41	3.88	1.04	0.05	0	0	0
Si–Na	4.7	3.72	2.15	6.99	23.60	32.76	23.40	10.59	2.34	0.33	0	0

TABLE 8 Cutoff and average radius, mean coordination, and coordination distribution of EGCa10 at 300 K

EGCa10	Cutoff *R* (Å)	Avg *R* (Å)	Avg Coord	0	1	2	3	4	5	6	7	8
Si–O	1.9	1.62	4.00	0	0	0	0	99.95	0.05	0	0	0
Al–O	2.3	1.77	4.23	0	0	0	0.58	76.24	22.44	0.74	0	0
B–O	1.9	1.39	3.23	0	0	0	76.57	23.43	0	0	0	0
Al–Ca	4.56	3.53	1.27	20.79	42.66	26.65	8.75	1.07	0.08	0	0	0
Al–Na	—	—	—	—	—	—	—	—	—	—	—	—
B–Ca	4.32	3.45	0.92	35.81	41.42	17.99	4.37	0.41	0	0	0	0
B–Na	—	—	—	—	—	—	—	—	—	—	—	—
Si–Ca	4.62	3.70	0.96	33.26	42.90	18.88	4.48	0.42	0.05	0	0	0
Si–Na	—	—	—	—	—	—	—	—	—	—	—	—

TABLE 9 Cutoff and average radius, mean coordination, and coordination distribution of EGCa20 at 300 K

$EGCa_{20}$	Cutoff *R* (Å)	Avg *R* (Å)	Avg Coord	0	1	2	3	4	5	6	7	8
Si–O	1.9	1.62	4.00	0	0	0	0	99.71	0.29	0	0	0
Al–O	2.3	1.76	4.25	0	0	0	0	74.88	24.88	0.24	0	0
B–O	1.9	1.42	3.46	0	0	0	54.00	46.00	0	0	0	0
Al–Ca	4.58	3.53	2.44	2.56	16.32	34.08	31.28	13.20	2.24	0.24	0.08	0
Al–Na	—	—	—	—	—	—	—	—	—	—	—	—
B–Ca	4.3	3.42	1.98	7.44	27.60	34.88	21.76	6.56	1.60	0.16	0	0
B–Na	—	—	—	—	—	—	—	—	—	—	—	–
Si–Ca	4.62	3.66	1.85	9.68	30.75	32.85	19.28	6.19	1.09	0.16	0	0
Si–Na	—	—	—	—	—	—	—	—	—	—	—	—

concentration of calcia and soda (10% each). This result agrees with observations made by Doweidar et al.[40] on Na_2O–Al_2O_3–B_2O_3 glasses. Na preferentially charge compensates the Al prior to charge compensating B, so increased Al_2O_3 at constant modifier content provides a mechanism for lowering the BO_4 content. At an equal concentration of calcia and soda, Wu and Stebbins similarly showed that increasing the Al_2O_3/B_2O_3 content (by lowering the B_2O_3 content) in alumino-borosilicates lowered the BO_4 content.[14]

Figure 3B shows that an increase in the Na_2O concentration increases the concentration of BO_4, whereas Ca has a lesser effect. The EGNa20, with 20% Na_2O and no CaO, has a BO_3/BO_4 ratio of ~0.61, whereas the EGCa20 and no Na_2O glass has a BO_3/BO_4 ratio of ~1.17. This is consistent with the idea that Na has a greater effect on the formation of BO_4 than does Ca. As the ratio of CaO/Na_2O increases, the ratio of BO_3/BO_4 increases, which is consistent with experimental results by Wu and Stebbins.[14,15] Figure 3B shows that there is no prominent BO_4 peak in

TABLE 10 Cutoff and average radius, mean coordination, and coordination distribution of EGNa10 at 300 K

$EGNa_{10}$	Cutoff *R* (Å)	Avg *R* (Å)	Avg Coord	0	1	2	3	4	5	6	7	8
Si–O	1.9	1.62	4.00	0	0	0	0	99.78	0.22	0	0	0
Al–O	2.3	1.77	4.27	0	0	0	0	73.64	25.43	0.94	0	0
B–O	1.9	1.40	3.27	0	0	0	73.04	26.96	0	0	0	0
Al–Ca	—	—	—	—	—	—	—	—	—	—	—	—
Al–Na	4.68	3.63	2.39	4.76	17.94	30.19	31.04	12.59	3.32	0.17	0	0
B–Ca	—	—	—	—	—	—	—	—	—	—	—	—
B–Na	4.54	3.55	1.88	9.86	30.36	31.29	20.66	6.29	1.36	0.17	0	0
Si–Ca	—	—	—	—	—	—	—	—	—	—	—	—
Si–Na	4.68	3.72	2.10	7.33	24.02	34.19	22.88	9.52	1.94	0.10	0.02	0

TABLE 11 Cutoff and average radius, mean coordination, and coordination distribution of EGNa20 at 300 K

$EGNa_{20}$	Cutoff *R* (Å)	Avg *R* (Å)	Avg Coord	0	1	2	3	4	5	6	7	8
Si–O	1.9	1.62	4.01	0	0	0	0	98.81	1.19	0	0	0
Al–O	2.3	1.76	4.25	0	0	0	0	75.85	23.64	0.51	0	0
B–O	1.9	1.44	3.62	0	0	0	37.93	62.07	0	0	0	0
Al–Ca	—	—	—	—	—	—	—	—	—	—	—	—
Al–Na	4.68	3.59	4.64	0	0.43	4.00	14.54	26.79	27.98	19.56	6.04	0.68
B–Ca	—	—	—	—	—	—	—	—	—	—	—	—
B–Na	4.54	3.50	4.07	0.43	1.96	8.33	20.66	30.95	25.85	9.95	1.45	0.43
Si–Ca	—	—	—	—	—	—	—	—	—	—	—	—
Si–Na	4.68	3.68	4.20	0.31	1.64	8.84	19.33	27.81	25.28	12.84	3.32	0.62

the B–O PDF for the compositions EGCa10 and EGNa10. Moreover, the ratios of BO_3/BO_4 for these compositions are ~3.27 and ~2.71, respectively. The two BO_3/BO_4 ratios are much higher than the ratio of BO_3/BO_4 for the compositions EGCa20, EGNa20, EGA5B15, EGA10B10, and EGA15B5, where the ratio does not exceed 1.2. The BO_3/BO_4 ratio of EGA10B10 is ~0.88. Taking into account the large difference in BO_3/BO_4 ratios between EGNa20 and EGCa20, as well as between EGNa10 and EGCa10, again

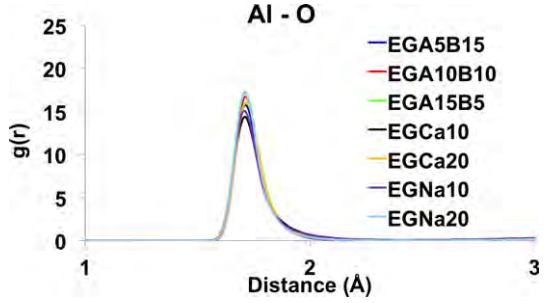

FIGURE 2 The Al–O bond distances at 300 K of samples EGA5B15, EGA10B10, EGA15B5, EGCa20, EGCa10, EGNa20, EGNa10 [Color figure can be viewed at wileyonlinelibrary.com]

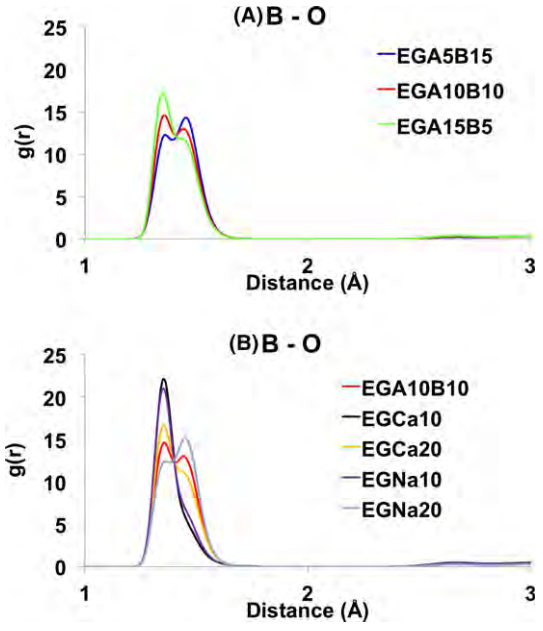

FIGURE 3 The B–O bond distances at 300 K of samples (A) EGA5B15, EGA10B10, EGA15B5, and (B) EGA10B10, EGCa20, EGCa10, EGCa10, EGNa20, EGNa10 [Color figure can be viewed at wileyonlinelibrary.com]

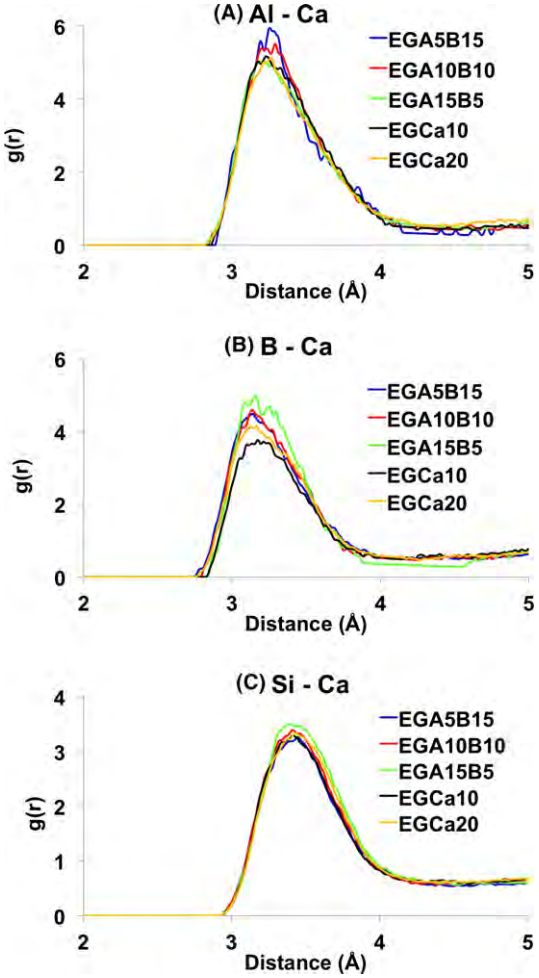

FIGURE 4 The (A) Al–Ca bond distances, (B) B–Ca bond distances, and (C) Si–Ca bond distances at 300 K of samples EGA5B15, EGA10B10, EGA15B5, EGCa20, EGCa10 [Color figure can be viewed at wileyonlinelibrary.com]

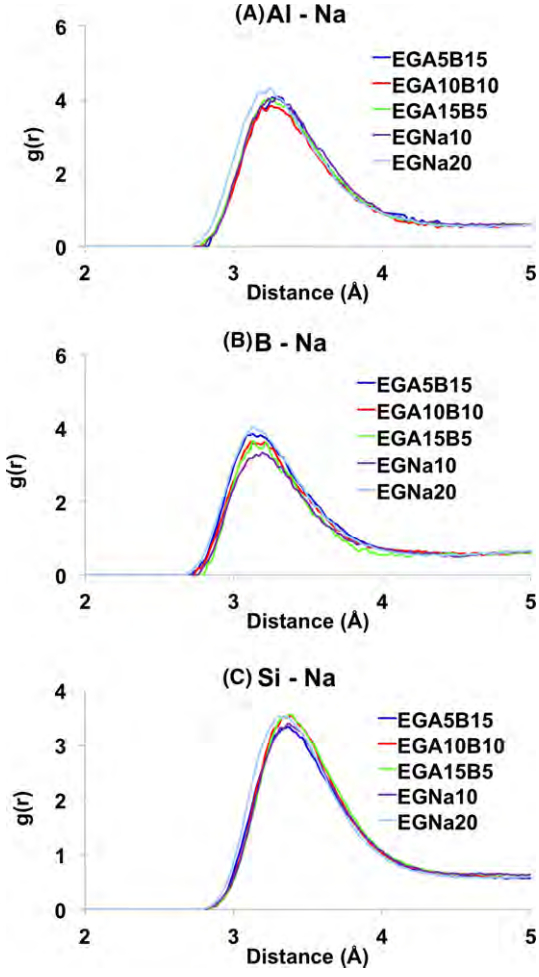

FIGURE 5 The (A) Al–Na bond distances, (B) B–Na bond distances, and (C) Si–Na bond distances at 300 K of samples EGA5B15, EGA10B10, EGA15B5, EGNa20, EGNa10 [Color figure can be viewed at wileyonlinelibrary.com]

Ca^{2+} is less effective in forming BO_4 over BO_3 than Na^+, again consistent with the Wu and Stebbins results.[14]

Table 4 shows that the Ca–O interatomic distances are noticeably less than that of Na–O, as expected. The interatomic distances between the network formers to the modifiers, Al/B–Ca and Al/B–Na, are about the same, whereas the Si–Ca and Si–Na have longer average interaction distances. Experimental data by Lee and Stebbins showed that the Na distance from the bridging oxygen in the Si–O–Si is longer than the bridges containing Al,[41] which would imply longer Si–Na distance than Al–Na.

Figures 4 and 5 show the PDFs for Al/B/Si–Ca/Na peak radii (first peak maximum in the PDF) for each composition. The Al–Ca peaks range between 3.21-3.29 Å, which is smaller than the 3.37 Å previously calculated using smaller system sizes.[12,19] Moreover, our Al–Ca and Si–Ca PDFs, found in Figure 4, show the existence of only one prominent peak for Si–Ca and Al–Ca bonds rather than two distinct peaks. Simulations by Benoit et al. and Ganster et al. predicted that there should be two close peaks in the Al–Ca and Si–Ca PDFs. This difference, however, is due to a larger system of atoms used in the current simulations, allowing for more local configurations. Our Si–Ca peaks range between 3.39-3.47 Å and agrees well with the range 3.40-3.50 Å found in the EXAFS data of calcium aluminosilicates.[33] The bond length ranges and the corresponding references can be found in Table 4.

Tables 5-11 also show the mean coordination and the distribution of the coordination of Al/B/Si–O/Ca/Na bonds, as well as the average radius of each bond. Tables 5-11 show the mean coordination of the following compositions: EGA5B15, EGA10B10, EGA15B5, EGNa10, EGNa20, EGCa10, and EGCa20, respectively. For the compositions containing Ca^{2+}, the mean coordination of Al–Ca is greater than that of B–Ca, which is greater than that of Si–Ca; this indicates that Ca^{2+} prefers to aggregate first around Al^{3+}, then B^{3+}, then Si^{4+}. Similarly, from these compositions containing Na^+, the mean coordination of Al–Na is greater

Journal of the American Ceramic Society

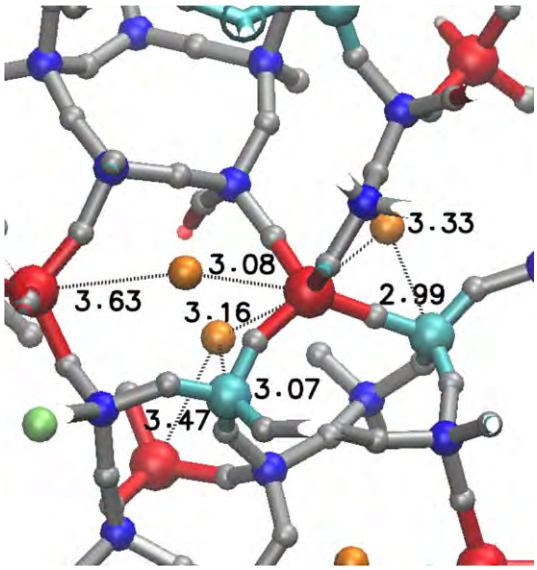

FIGURE 6 Interaction distances between Na ions (orange) and Al (red) or B (cyan). Si (blue), O (gray), Ca (lime). Most Na-(Al,B) distances are less than 4 Å, showing multiple Na neighbors to a single Al, but also multiple +3 cations to a single Na [Color figure can be viewed at wileyonlinelibrary.com]

than that of Si–Na, which is greater than that of B–Na; this indicates that Na^{+} prefers to aggregate first around Al^{3+}, then Si^{4+}, then B^{3+}, consistent with experimental results.[42]

For all compositions, the mean coordination of the network formers to Na (Al/B/Si–Na) is about twice that of the formers to Ca (Al/B/Si–Ca), as shown in Tables 5-11. The data given in the tables are dependent on the cut-off distance, which is chosen as the first minimum in the relevant PDFs. It is common to describe the interaction between a modifier and the +3 cations such as Al or B in the +4 Si site as being one Na per +3 cation and one Ca for 2 nearby +3 cations. Therefore, it would appear inconsistent that there are, on average, 2 Na near Al and B (and Si) and 1 Ca per Al or B. However, the simplistic consideration of charge compensation usually assumed is correct with regard to the ratio of mole fractions of +1 or +2 modifiers to +3 cations, but not with respect to physical location of the modifiers. Figure 6 provides a snapshot of the local configuration of Na near Al and B atoms in the EGA10B10 glass. As the figure shows, one Al ion can have multiple Na within 4 Å, but also the Na can be within 4 Å of several +3 cations. This is possible with the relatively high concentrations of Al and B that show some degree of clustering in this glass caused by the presence of the higher cation field strength Ca ions that reduces the so-called Al or B avoidance.[11,43] Multiple interaction distances with the Na or Ca ions are observed for the Na–O and Ca–O interactions also. As previously discussed in simulations and EXAFS results regarding binary sodium silicates, a Na ion may draw close to an NBO while it is also interacting with the BO nearby.[24,29] In the multicomponent glasses studied in this article, the Na or Ca near the +3 cations interact with multiple BO, as shown in Figure 7. Such results in Figures 6 and 7 indicate a structural complexity that would be relevant in the structural models describing the mixed alkali effect, where modifier-former interactions create local structures relevant to the modifier that are influenced by the location of the network formers.

From the samples EGA5B15, EGA10B10, and EGA15B15, it can be shown that the mean coordination for Al–Ca is about half of that for Al–Na; similarly the mean coordination of B–Ca is about half that of B–Na. The mean coordination of Si–Ca is less than that of Si–Na. In addition to the mean coordinations, Tables 5-11 indicate that the concentration of Al with no (0) Ca neighbors is much higher than the Al with no Na neighbors, indicating the stronger preference for Al to interact with Na over Ca.

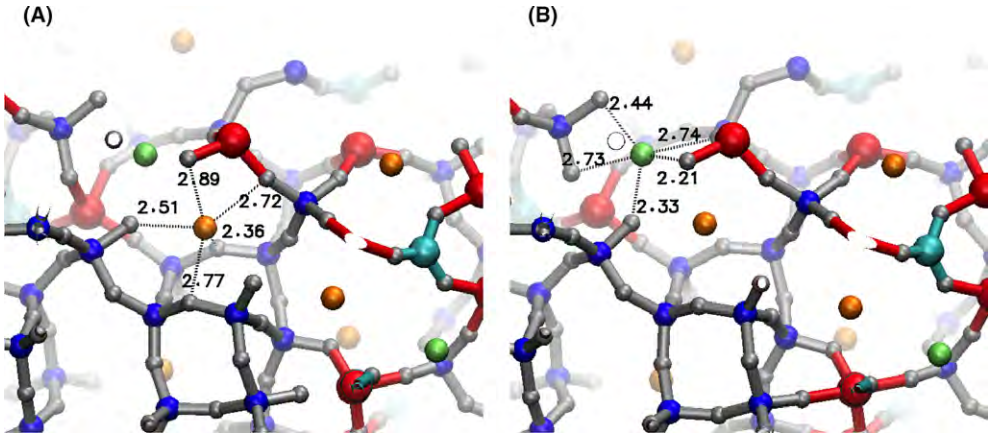

FIGURE 7 (A) Na–O interaction distances and (B) Ca–O interaction distances at an instant in the simulations. Color scheme as in Figure 6. The Na-Ca spacing fluctuates near 3.2 Å. Not all former-oxygen bonds are included in the figure since atoms have been removed for clarity of the image [Color figure can be viewed at wileyonlinelibrary.com]

Si and B behave similarly, although increasing the concentration of Al_2O_3 affects behavior with B. The mean coordination of B–Na relative to that of B–Ca decreases as the Al_2O_3/B_2O_3 ratio increases; the ratio of the mean coordination of B–Na to that of B–Ca is ~2.01 for EGA5B15, ~1.91 for EGA10B10, and ~1.71 for EGA15B5. This is consistent with the preferential distribution of Na with Al prior to Si prior to B, referenced above.

The correlations between the decreasing preference for B^{3+} to interact with Na^{2+} with increasing Al_2O_3 and between the direct relationship that increasing the Al_2O_3/B_2O_3 ratio causes the increase in the BO_3/BO_4 ratio indicates that the network former around which a modifier aggregates affects the BO_3/BO_4 ratio. These results suggest that the loss of Na near B with increasing Al_2O_3 enables a stronger role for Ca and its higher cation field strength to affect the BO_3/BO_4 ratio. This is consistent with experimental results of soda-lime-alumino-borosilicate glass compositions.[15,17] This suggests that where the Ca^{2+} modifiers accumulate strongly affects the ratio of BO_3/BO_4 and that the ratio of Al_2O_3/B_2O_3 indirectly influences where Ca^{2+} atoms aggregate.

4 | CONCLUSION

The structure of alumino-borosilicate glasses was studied using samples of varying compositions containing ~20 000 atoms each. PDFs of cations to oxygen, Si/Al/B/Ca/Na–O, were used for comparison to available experimental data to evaluate consistency between simulations and experiment. Additional PDFs and coordination of the network forming cations (Al/B/Si) to network modifiers (Ca/Na) were examined, the latter of which is difficult to measure experimentally. As discussed throughout the text, the results are consistent with available experimental data regarding bond lengths and network former to oxygen coordination numbers. Si is predominantly 4-coordinated, with a small concentration of 5-coordinated Si. Al is also predominantly 4-coordinated, with some 5-coordinated Al and a very minor amount of 6 coordinated Al. The most variable structure occurred with B coordination, which is affected by the Na preference for Al prior to the other network formers that lowers Na aggregation near B which affects B coordination. B varied as 3-coordinated, BO_3, and 4-coordinated, BO_4, units as a function of the amount of Ca^{2+} and Na^+ present, the ratio of Al_2O_3 to B_2O_3, and the fictive temperature of the sample, similar to experimental data.

Given the similarity of the simulations to the experimental data described above, the simulations provide new information regarding the locations on the network modifiers to the +3 cations, Al and B. Unlike the simple idea based on stoichiometry of associating one +1 network modifier with one +3 network former, the simulations indicate that the modifiers associate with multiple +3 cations and vice versa. For instance, one Al ion can have multiple Na within 4 Å, but also the Na can be within 4 Å of several +3 cations. Stoichiometry is maintained, but structure is more complex and would manifest itself in the various structural models of the mixed alkali effect where modifier-former interactions create local structures relevant to the modifier that are influenced by the location of the network formers.

REFERENCES

1. Barinov D, Smakota N, Ponomarchuk S, Akhmetshina A, Kozlova A. Cover-coat enamels based on alkali calcium aluminoborosilicate glasses. *Glass Ceram*. 1972;29:733–735.
2. Kudryavtsev M, Kolesov YI, Mikhailenko NY. Boron-free, alkali-free glass fibre for production of fibreglass-reinforced plastics. *Fibre Chem*. 2001;33:242–244.
3. Malchukova E, Boizot B. β-irradiation effect in aluminoborosilicate glasses: the role of RE codoping (RE = Sm, Gd). *Phys Sol State*. 2008;50:1687–1691.
4. Mashir YI. Optimization of the matrix compositions and properties of silver-free photochromic glasses. *Glass Ceram*. 1997;54:267–270.
5. Zhang M, Matinlinna JP. E-glass fiber reinforced composites in dental applications. *Silicon*. 2012;4:73–78.
6. Dong C, Davies IJ. Flexural properties of E glass and TR50S carbon fiber reinforced epoxy hybrid composites. *J Matl Eng Perform*. 2013;22:41–49.
7. Oguni K, Ravichandran G. Dynamic compressive behavior of unidirectional E-glass/vinylester composites. *J Matl Sci*. 2001;36:831–838.
8. Promis G, Bach T, Gabor A, Hamelin P. Failure behavior of E-glass fiber-and fabric-reinforced IPC composites under tension and compression loading. *Matls Struct*. 2014;47:631–645.
9. Cormack AN, Cao Y, Molecular dynamics simulation of silicate glasses. In: Silvi B, D'Arco P, eds. *Modelling of Minerals and Silicated Minerals, Vol. 15. Topics in Molecular Organization and Engineering*. Dordrecht, The Netherlands:Kluwer Academic; 1997:227–271.
10. Darwish H, Gomaa M. Effect of compositional changes on the structure and properties of alkali-alumino borosilicate glasses. *J Matl Sci*. 2006;17:35–42.
11. Du L-S, Stebbins JF. Network connectivity in aluminoborosilicate glasses: a high-resolution ^{11}B, ^{27}Al and ^{17}O NMR study. *J Non-Cryst Sol*. 2005;351:3508–3520.
12. Ganster P, Benoit M, Kob W, Delaye J-M. Structural properties of a calcium aluminosilicate glass from molecular-dynamics simulations: a finite size effects study. *J Chem Phys*. 2004;120:10172–10181.
13. Manara D, Grandjean A, Neuville D. Advances in understanding the structure of borosilicate glasses: a Raman spectroscopy study. *Am Miner*. 2009;94:777–784.
14. Wu J, Stebbins JF. Effects of cation field strength on the structure of aluminoborosilicate glasses: high-resolution ^{11}B, ^{27}Al, and ^{23}Na MAS NMR. *J Non-Cryst Sol*. 2009;355:556–562.
15. Wu J, Stebbins JF. Temperature and modifier cation field strength effects on aluminoborosilicate glass network structure. *J Non-Cryst Sol*. 2013;362:73–81.

16. Bray PJ, Geissberger AE, Bucholtz F, Harris IA. Glass structure. *J Non-Crys Sol*. 1982;52:45–66.
17. Du L-S, Stebbins JF. Site preference and Si/B mixing in mixed-alkali borosilicate glasses: a high-resolution ^{11}B and ^{17}O NMR study. *Chem Matls*. 2003;15:3913–3921.
18. Thompson LM, Stebbins JF. Non-stoichiometric non-bridging oxygens and five-coordinated aluminum in alkaline earth aluminosilicate glasses: effect of modifier cation size. *J Non Cryst Sol*. 2012;358:1783–1789.
19. Benoit M, Profeta M, Mauri F, Pickard CJ, Tuckerman ME. First-principles calculation of the ^{17}O NMR parameters of a calcium aluminosilicate glass. *J Phys Chem B*. 2005;109:6052–6060.
20. Blonski S, Garofalini SH. Atomistic structure of calcium silicate intergranular films in alumina studied by molecular dynamics simulations. *J Am Ceram Soc*. 1997;80:1997–2004.
21. Litton DA, Garofalini SH. Atomistic structure of sodium and calcium silicate intergranular films in alumina by molecular dynamics. *J Mater Res*. 1999;14:1418–1429.
22. Zhang S, Garofalini SH. Molecular dynamic computer simulations of the interface structure of calcium-alumino-silicate intergranular films between combined basal and prism planes of a-Al_2O_3. *J Am Ceram Soc*. 2005;88:202–209.
23. Blonski S, Garofalini SH. Molecular dynamics simulations of a-alumina and g-alumina surfaces. *Surf Sci*. 1993;295:263–274.
24. Melman H, Garofalini SH. Microstructural evaluation of simulated sodium silicate glasses. *J Non-Cryst Solids*. 1991;134:107–115.
25. Feuston BP, Garofalini SH. Empirical three-body potential for vitreous silica. *J Chem Phys*. 1988;89:5818–5824.
26. Zirl DM, Garofalini SH. Structure of sodium-aluminosilicate glasses. *J Am Ceram Soc*. 1990;73:2848–2856.
27. Garofalini SH, Molecular dynamics simulations of glass surfaces and interfaces. In: *Reviews in Mineralogy and Geochemistry: Molecular Modeling Theory: Applications to the Geosciences, Vol. 42*. Cygan R, Kubicki J, eds. Washington D. C.:Mineralogical Society of America; 2001:131–164.
28. Adelstein N, Olsen CS, Lordi V. Hole traps in sodium silicate: first-principles calculations of themobility edge. *J Non-Cryst Sol*. 2015;430:9–15.
29. Greaves GN, Fontaine A, Lagarde P, Raoux D, Gurman SJ. Local structure of silicate glasses. *Nature*. 1981;293:611–616.
30. Stebbins JF, McMillan P. Compositional and temperature effects on five-coordinated silicon in ambient pressure silicate glasses. *J Non Cryst Sol*. 1993;160:116–125.
31. Stebbins JF. NMR evidence for five-coordinated silicon in a silicate glass at atmospheric pressure. *Nature*. 1991;351:638–639.
32. Lloyd L. *Fundamental and Applied Catalysis, Handbook of Industrial Catalysis*. New York City, New York: Springer; 2011: ISBN 978-0-387-24682-6.
33. Brown G, Waychunas G, Ponader C, Jackson W, McKeown D. EXAFS and NEXAFS studies of cation environments in oxide glasses. *J de Physique*. 1986;C8–661–C8-C68.
34. Cormier L, Neuville DR, Calas G. Structure and properties of low-silica calcium aluminosilicate glasses. *J Non-Cryst Solids*. 2000;274:110–114.
35. Schmücker M, Schneider H, MacKenzie K, Okuno M. Comparative ^{27}Al NMR and LAXS studies on rapidly quenched aluminosilicate glasses. *J Eur Ceram Soc*. 1999;19:99–103.
36. Wu J, Stebbins JF. Quench rate and temperature effects on boron coordination in aluminoborosilicate melts. *J Non-Cryst Sol*. 2010;356:2097–2108.
37. Biscoe J, Warren B. X-ray diffraction study of soda-boric oxide glass. *J Am Ceram Soc*. 1938;21:287–293.
38. Emme H, Huppertz H. High-pressure preparation, crystal structure, and properties of α-(RE) $2B_4O_9$ (RE= Eu, Gd, Tb, Dy): oxoborates displaying a new type of structure with edge-sharing BO_4 tetrahedra. *Chem A Eur J*. 2003;9:3623–3633.
39. Soules T. A molecular dynamics calculation of the structure of B_2O_3 glass. *J Chem Phys*. 1980;73:4032–4036.
40. Doweidar H, Moustafa Y, El-Maksoud SA, Silim H. Properties of Na_2O–Al_2O_3–B_2O_3 glasses. *Matls Sci Eng A*. 2001;301:207–212.
41. Lee SK, Stebbins JF. The distribution of sodium ions in aluminosilicate glasses: a high-field Na-23 MAS and 3P MAS NMR study. *Geochim Cosmochim Acta*. 2003;67:1699–1709.
42. El-Damrawi G, Muller-Warmuth W, Doweidar H, Gohar IA. ^{11}B, ^{29}Si, and ^{27}Al nuclear magnetic resonance studies of Na_2O-Al_2O_3-B_2O_3-SiO_2 glasses. *Phys Chem Glasses*. 1993;34:52–57.
43. Lee SK, Stebbins JF. The structure of aluminosilicate glasses: high-resolution ^{17}O and ^{27}Al MAS and 3QMAS NMR study. *J Phys Chem B*. 2000;104:4091–4100.
44. Soules T. A molecular dynamic calculation of the structure of sodium silicate glasses. *J Chem Phys*. 1979;71:4570–4578.
45. Navrotsky A, Geisinger KL, McMillan P, Gibbs GV. The tetrahedral framework in glasses and melts - inferences from molecular orbital calculations and implications for structure, thermodynamics, and physical properties. *Phys Chem Miner*. 1985;11:284–298.
46. Cormier L, Neuville D. Ca and Na environments in Na_2O–CaO–Al_2O_3–$SiOS_2$ glasses: influence of cation mixing and cation-network interactions. *Chem Geo*. 2004;213:103–113.
47. Merzbacher C, White WB. Structural of Na in aluminosilicate glasses: a far-infrared reflectance spectroscopic study. *Am Miner*. 1988;73:1089–1094.

SUPPORTING INFORMATION

Additional Supporting Information may be found online in the supporting information tab for this article.

How to cite this article: Ha MT, Garofalini SH. Local structure of network modifier to network former ions in soda-lime alumino-borosilicate glasses. *J Am Ceram Soc*. 2017;100:563-573.